

# Macromolecules

Volume 25, Number 24

November 23, 1992

© Copyright 1992 by the American Chemical Society

## Influence of Molecular Weight on the Melting and Phase Structure of Random Copolymers of Ethylene

R. G. Alamo, E. K. M. Chan,<sup>†</sup> and L. Mandelkern\*

*Department of Chemistry and Institute of Molecular Biophysics, Florida State University, Tallahassee, Florida 32306*

I. G. Voigt-Martin

*Institut für Physikalische Chemie, Johannes-Gutenberg Universität, D-65 Mainz, Germany*

*Received April 28, 1992; Revised Manuscript Received August 14, 1992*

**ABSTRACT:** The melting temperatures and phase structures of a series of hydrogenated polybutadienes with fixed co-unit content (2.3 mol % branch points) and varying molecular weights have been studied. These copolymers represent molecular weight and composition fractions of randomly ethyl-branched ethylene copolymers. Also studied were a set of random ethylene-hexene copolymers with a lower co-unit content. The observed melting temperatures, after a variety of crystallization procedures, were found to decrease with increasing molecular weight for both copolymer types. This unusual result could be attributed to the decreasing crystallite thickness in the chain direction with molecular weight. At the higher molecular weights,  $M = 4.6 \times 10^5$ , the crystallite thickness is reduced to about 30 Å. Associated with the crystallite is a relatively large disordered overlayer. Although small-angle X-ray measurements and thin-section transmission electron microscopy give results that are in quantitative agreement for the crystallite thickness, the Raman LAM measurement give significantly higher values in the low-size range. The conventional extrapolative method of plotting the observed melting temperature against the crystallization temperature, in order to obtain the equilibrium melting temperature, failed for the random copolymers at low levels of crystallinity. A straight line resulted that paralleled the 45° line. Therefore, extrapolation to the equilibrium melting temperature could not be accomplished. Although the extrapolation could be made for higher levels of crystallinity, this procedure was arbitrary and lead to unreasonable values for the equilibrium melting temperature.

### Introduction

Many properties of crystalline polymers are known to be very dependent on molecular weight and crystallization conditions.<sup>1-5</sup> Linear polyethylene has been extensively studied in this connection. A variety of properties ranging from simple thermodynamic to more complex mechanical ones follow this generalization.<sup>2-15</sup> The reason for the change in properties is that the fundamental structural features, which define and describe the crystalline state, can be varied over wide limits by control of molecular weight and crystallization conditions. Random copolymers would be expected to behave in a similar manner. With copolymers, besides molecular weight and crystallization conditions, the influence of co-unit type and concentration needs to be assessed. Although many properties of copolymers have been investigated, there is a lack of studies where molecular weight and co-unit content are controlled. We report here a detailed study and analysis of the melting temperature and phase structure of a set of random ethylene copolymers where both the molecular weight and

composition are controlled. We have chosen for study a set of copolymers for which it has already been established that the co-units do not enter the crystal lattice.<sup>16-21</sup> With these samples it is possible to independently assess the influence of molecular weight and of copolymer composition on the properties of interest.

### Experimental Section

**Materials.** The molecular characteristics of the random ethylene copolymers used in this work are listed in Table I. The hydrogenated polybutadienes, labeled HPBD, were supplied by Dr. William W. Graessley; their synthesis and some of their properties have been previously given.<sup>22,23</sup> Samples designated P-16, P-108, and P-420 are also hydrogenated polybutadienes that were purchased from the Phillips Chemical Co. These copolymers have narrow molecular weight and composition distributions. The ethylene-1-hexene copolymers studied in this work were prepared by the method of Kaminsky et al.<sup>24</sup> using  $(C_5H_5)_2ZrCl_2$  as catalyst. These copolymers have a most probable molecular weight and narrow composition distributions.<sup>25</sup> The ethylene-1-octene is a fraction that has been used in a previous work.<sup>17</sup> The details of the fractionation procedure have also been given.<sup>17</sup> A fraction of a high-pressure free-radical polymerized ethylene, containing both long-chain and short-chain branches,

<sup>†</sup> Baxter Healthcare Corp., Baxter Technology Park, Round Lake, IL 60073.

Table I  
Molecular Characteristics of Ethylene Copolymers

copolymer type	designation	$M_w \times 10^{-3}$	$M_w/M_N$	IR	$^{13}\text{C}$ NMR
hydrogenated PBD	HPBD-2200	2.2	$\approx 1.1$	2.16	
hydrogenated PBD	HPBD-3580	3.58	$\approx 1.1$	2.30	2.15
hydrogenated PBD	HPBD-4530	4.53	$\approx 1.1$	2.27	
hydrogenated PBD	HPBD-6950	6.95	$\approx 1.1$	2.36	
hydrogenated PBD	P-16	16	1.4	2.10	2.05
hydrogenated PBD	HPBD-24	24	$\approx 1.1$	2.30	
hydrogenated PBD	HPBD-79	79	$\approx 1.1$	2.44	
hydrogenated PBD	P-108	108	1.31	2.20	2.08
hydrogenated PBD	HPBD-145	145	$\approx 1.1$	2.70	
hydrogenated PBD	P-420	420	1.84	2.20	
hydrogenated PBD	HPBD-460	460	$\approx 1.1$	2.36	
hydrogenated PBD	HPBD-4	160	1.05		3.2
hydrogenated PBD	HPBD-5	180	1.05		4.5
hydrogenated PBD	HPBD-6	150	1.05		5.75
ethylene-1-hexene	EH-19	18.9	2.39	1.43	
ethylene-1-hexene	EH-112	112	2.0	1.48	
ethylene-1-hexene	EH-240	240	2.17	1.47	
ethylene-1-hexene	EOA-1	$\approx 60$		0.69	
branched PE (high pressure)	A-5	123			1.01

was also used in some experiments.<sup>26</sup> It contained a total branching content of 1.01 mol %. The branching content of all the copolymers was measured by IR spectroscopy using a calibration established by  $^{13}\text{C}$  NMR. Some of the samples were also directly analyzed by  $^{13}\text{C}$  NMR.<sup>27,28</sup> The results from both kinds of spectroscopy were similar and are also listed in Table I. The weight- and number-average molecular weights were obtained by gel permeation chromatography following conventional procedures.

**Procedures.** Melting temperatures were obtained in a Perkin Elmer DSC-2B differential scanning calorimeter operating at a heating rate of 10 °C/min. The melting points were identified with the maximum in the endothermic peak. To avoid differences in melting temperatures caused by variations in sample weight, a sample mass of about 3 mg was used in all the DSC experiments. In a majority of the experiments a rapid quenching crystallization procedure was adapted to ensure similar kinetics and morphology. In this procedure a thin film, placed between aluminum foil, was immersed in an oven at 150 °C for approximately 2 min and then dropped quickly into a dry ice/2-propanol mixture set at -78 °C. This method ensures a very efficient quenching. The resulting quenched films of about 150  $\mu\text{m}$  thick were used in the DSC experiments, density, X-rays, Raman spectroscopy, and transmission electron microscopy. In a specific set of experiments the hydrogenated polybutadienes were crystallized isothermally at higher temperatures in order to better approach equilibrium conditions. The crystallization temperature was chosen to correspond to the maximum in the exothermic peak obtained when the sample was cooled in the DSC at 5 °C/min. The samples were held at this temperature for 16 h and then heated at the rate of 10 °C/min. The enthalpies of fusion were calculated from the area of the melting endotherm and converted to degrees of crystallinity,  $(1 - \lambda)_{\Delta H}$ , by taking the enthalpy of a perfect polyethylene crystal to be 69 cal/g.<sup>29</sup>

The melting behavior of the hydrogenated polybutadienes with molecular weights between 6950 and 460 000 and constant branching content of about 2.3 mol % were also studied by standard dilatometric methods.<sup>4,30,31</sup> Conventional dilatometers with sample weights of about 0.2 g were used.<sup>31</sup> Details concerning the preparation of the dilatometer and of the crystallization procedures have been described in a previous publication.<sup>32</sup> The melting process was followed from the isothermal crystallization temperature after the maximum extent of the transformation was attained. A slow heating rate was adopted particularly in the temperature interval close to melting. The complete melting process usually took 8–10 days.

The densities were measured at 23 °C in a triethylene glycol/2-propanol density gradient column calibrated with standard glass floats. The densities were converted to degrees of crystallinity  $(1 - \lambda)_d$  by the specific volume relationship given by Chiang and Flory.<sup>33</sup>

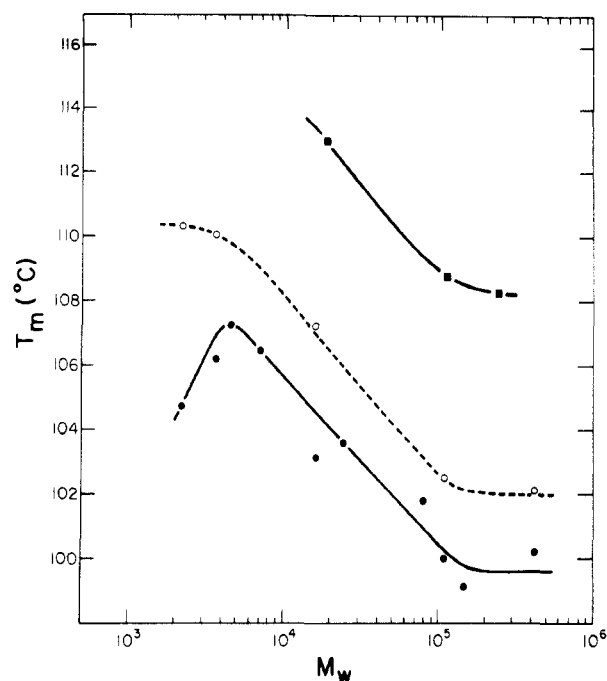


Figure 1. Plot of melting temperature,  $T_m$ , against log weight average molecular weight,  $M_w$ , for hydrogenated polybutadienes ( $\sim 2.3$  mol % branch points) and ethylene-hexene copolymers ( $\sim 1.45$  mol % branch points). Hydrogenated polybutadienes:  $\bullet$ , rapidly crystallized;  $\circ$ , pseudo isothermally crystallized. Ethylene-hexene:  $\blacksquare$ , rapidly crystallized.

Small-angle X-ray scattering patterns of the quenched films were photographically recorded using a slit-collimated Rigaku-Denki camera and Cu K $\alpha$  radiation with exposure times of 24 h. The observed first-order maxima were converted to lamellar thickness by direct application of Bragg's law.

The staining and thin-sectioning techniques used in the transmission electron microscopy were similar to those described by Kanig.<sup>34,35</sup> Under carefully controlled conditions the staining agent penetrates only into the noncrystalline region which thus appear dark in the micrographs. Low staining temperatures (20 °C) and short staining times (12 h) have proven to give excellent results with other ethylene copolymers<sup>36</sup> so that these were the conditions used in the present work. Furthermore, comparison with correlation functions from X-ray work indicated that the crystalline thicknesses of a high-pressure polymerized polyethylene having 3.3 total branches per 100 carbons corresponds to a highly oriented core plus a less oriented surface region.<sup>21,37</sup>

The Raman spectra in the region 950–1550  $\text{cm}^{-1}$  as well as the longitudinal acoustic modes (LAM) were obtained by using instrumentation that has been previously described.<sup>8</sup> The method of analysis has also been described in detail.<sup>8,38–40</sup> In particular the ordered sequence length,  $L$ , was obtained from the LAM frequency,  $\Delta\bar{\nu}$ , by using the first term in the Shimanouchi-Schaufele relation<sup>40</sup> corrected for temperature:<sup>41</sup>

$$\Delta\bar{\nu} = \frac{m}{2cL} \left( \frac{E}{\rho} \right)^{1/2} \quad (1)$$

Here  $\Delta\bar{\nu}$  is the mode frequency,  $m$  is the mode order ( $m = 1, 3, 5, \dots$ ),  $c$  is the velocity of light,  $\rho$  the density of the vibrating ordered sequences, and  $E$  the Young's modulus in the chain direction.

## Results and Discussion

**Melting Behavior.** The melting temperatures as a function of molecular weight are plotted in Figure 1 for the hydrogenated polybutadienes containing about 2.3 mol % branch points and the ethylene-1-hexene copolymers with 1.45 mol % branch points. Both type of copolymers were rapidly crystallized (quenched) prior to fusion. The hydrogenated polybutadienes were also crystallized isothermally following the procedure described in the ex-

perimental part. Except for the quenched hydrogenated polybutadienes of the lowest molecular weight, where there is the distinct possibility of end-group effects, the melting temperatures decrease with increasing molecular weight. This decrease is especially marked in the  $10^4$ – $10^5$  molecular weight region where a decrease of the order of 7–8 °C is observed. A qualitatively similar set of results has been reported.<sup>42</sup> However, this behavior, and its significance, was not investigated further. The melting temperatures of the ethylene–hexene copolymers are displaced to higher values compared to the hydrogenated polybutadienes because of their lower co-unit content.<sup>17,25</sup> However, the molecular weight dependence of both copolymer types is very similar. The melting temperatures of the hydrogenated polybutadienes that were crystallized at elevated temperatures are plotted as the dashed curve in this figure. These data are displaced to higher values because of the higher crystallization temperatures. The trend with molecular weight is the same. We can conclude that the molecular weight effect on the melting temperature is quite general for random ethylene copolymers. The results illustrated in Figure 1 are unusual, since melting temperatures are expected to increase with molecular weight for both homopolymers and copolymers.<sup>43,44</sup> We thus need to seek the reason for this behavior.

The variation of the melting temperatures with molecular weight does not depend on the chemical nature of the co-unit for random copolymers.<sup>45</sup> The melting temperatures of copolymers are crucially dependent on the sequence distribution.<sup>17,43,44</sup> Hence, the possibility of the sequence distribution varying with molecular weight was investigated. Detailed <sup>13</sup>C NMR analysis were carried out for this specific purpose with three of the hydrogenated polybutadienes,  $M_w = 3580$ ,  $M_w = 16\,000$ , and  $M_w = 108\,000$ . The spectral data were analyzed according to the methods described by Randall.<sup>27,28,46</sup> It was found that they all possess a random sequence distribution. Possible differences in sequence distributions between the copolymers is, therefore, not the cause of the inversion of the melting temperatures.

The properties of the molecular chain constitution, chemical type co-unit, and sequence distribution, are not the cause of the molecular weight dependence. The reasons might be found in the changes with molecular weight of the crystallite structure and associated morphology. Before examining this possibility, it is of interest to establish the equilibrium melting temperature by extrapolation methods.

**Relation between Melting Temperature and Crystallization Temperature.** Because of the unusual results that have been described, an effort was made to establish the equilibrium melting temperature of each copolymer by an extrapolative method. An attractive and commonly used method is to determine the melting temperature,  $T_m$ , as a function of the crystallization temperature,  $T_c$ , and extrapolate the results to the intersection with the  $T_m = T_c$ , 45° straight line.<sup>47–49</sup> We shall term this the  $T_m/T_c$  method. This method has been very successful in determining the equilibrium melting temperature,  $T_m^\circ$ , for a variety of homopolymers.<sup>48,50–52</sup> According to the theory underlying this method (cf. below), as well as in practice, the experimental  $T_m$  should be determined only at very low levels of crystallinity.<sup>50,52</sup> This extrapolative method is based on the concept that the crystallite thickness, and thus the melting temperature, is related to the crystallization temperature by the dimensions of the critical size nucleus. The development of appreciable levels of crystallinity, at a given temperature, vitiates the basic postulate

Table II  
Samples Used for  $T_m$ – $T_c$  Experiments in Figure 2

symbol in Figure 2	copolymer type	mol % branch pts	$M_w$ $\times 10^{-4}$	$M_w/M_n$
×	linear polyethylene fraction	0	47 <sup>a</sup>	
▽	ethylene–1-hexene	0.42	≈7	
▼	ethylene–1-octene	0.69	≈7	
△	high-pressure branched PE (A5)	1.01	12.3	
▲	ethylene–vinyl acetate	1.12	7.1	4.4
○	hydrogenated polybutadiene	2.20	10.8	1.3
●	hydrogenated polybutadiene	2.20	42	2.66
□	ethylene–1-butene	2.64	10.6	2.7
■	hydrogenated polybutadiene	4.14	5	≈1.1
◻	hydrogenated polybutadiene	4.50	18	1.05

<sup>a</sup>  $M_n$  from ref 50.

underlying the method. This conclusion has been amply verified in the study of homopolymers.<sup>50,52</sup>

To apply this extrapolative method to the problem at hand, we have selected a comprehensive set of copolymer fractions for study. The characteristics of these copolymers are listed in Table II. They represent a wide range in co-unit type, co-unit concentration, and molecular weight. These copolymers were crystallized isothermally inside the DSC at a specified temperature for a predetermined time so that a crystallinity level of about 5% was attained. After this level of crystallinity was reached, the samples were heated at the rate of 10 °C/min, and the melting temperature  $T_m$  was determined. The directly observed melting temperature, obtained under these conditions, is plotted against the crystallization temperature in Figure 2. The results for all the copolymers listed in Table II are included in this figure. Also plotted, for reference purposes, are previously reported results for a linear polyethylene fraction that was initially crystallized to the same low crystallinity level.<sup>50</sup>

The plots in Figure 2 are quite surprising and not typical of the usual results obtained by this method. Each of the copolymers yields a straight line that is parallel to the  $T_m$ – $T_c$  line. The melting temperature and crystallization temperature decrease with co-unit content, as expected. However, as the dashed line indicates, despite the very large differences in the molecular constitution of the copolymers, they all fall on the same master straight line, with just minor deviations of the two copolymers with very high co-unit content. The expected, more conventional behavior is demonstrated by the polyethylene fraction. It is clear from these plots that an extrapolation to the equilibrium melting temperature of any of the copolymers by the prescribed method is operationally impossible.

Although these results do not represent the usual behavior there are several examples in the literature that are similar. Okui and Kawai have studied  $T_m/T_c$  extrapolations for ethylene–vinyl acetate copolymers.<sup>53</sup> Except for the very high crystallization temperatures, two melting peaks were observed. The lower melting temperatures resulted in straight lines parallel to the line  $T_m = T_c$ . The higher melting temperatures gave slopes between 0.35 and 0.50. Although the authors related the lower melting peak as a melting of a bundlelike crystal and the higher melting peak as coming from a folded lamellar crystal, the fact is that the copolymers that they investigated were not fractionated and the multiple melting behavior might be the result of a bimodal sequence distribution of the samples analyzed.

Lee and Porter reported two melting peaks for poly(ether ether ketone).<sup>54</sup> The lowest peak was parallel to the  $T_m$ – $T_c$  line and assigned to the thickened original

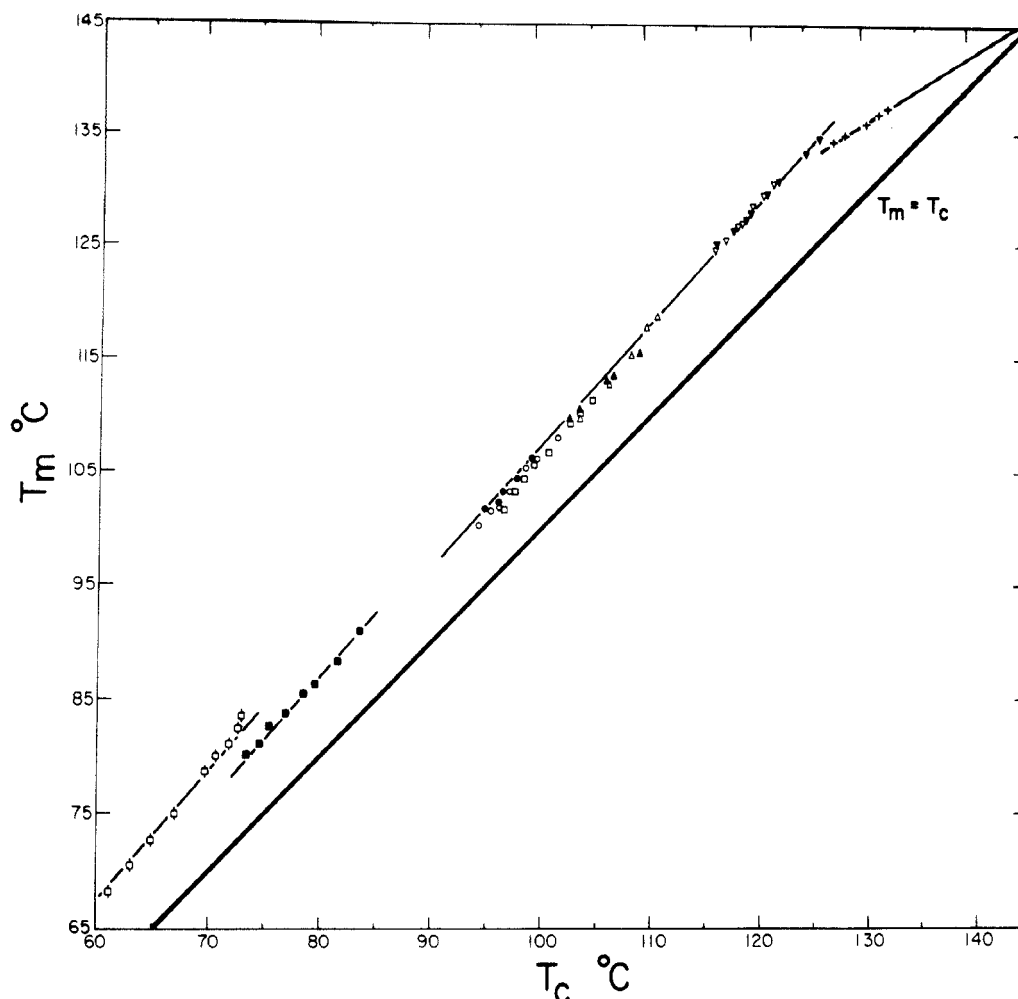


**Figure 2.** Plot of observed melting temperature against crystallization temperature for a series of random ethylene copolymer fractions and a linear polyethylene:  $\nabla$ , ethylene-butene, 0.42 mol % branch points,  $M_w \sim 7 \times 10^4$ ;  $\triangledown$ , ethylene-octene, 0.69 mole % branch points,  $M_w \sim 7 \times 10^4$ ;  $\Delta$ , high-pressure polymerized, branched polyethylene, 1.01 mol % branch points,  $M_w = 1.2 \times 10^5$ ;  $\triangle$ , ethylene-vinyl acetate, 1.12 mol % branch points,  $M_w = 7.1 \times 10^4$ ;  $\circ$ , hydrogenated polybutadiene, 2.20 mol % branch points,  $M_w = 1.08 \times 10^5$ ;  $\bullet$ , hydrogenated polybutadiene, 2.20 mol % branch points,  $M_w = 4.2 \times 10^5$ ;  $\square$ , ethylene-butene, 2.64 mol % branch points,  $M_w = 1.06 \times 10^5$ ;  $\blacksquare$ , hydrogenated polybutadiene, 4.10 mol % branch points,  $M_w = 5 \times 10^4$ ;  $\boxplus$ , hydrogenated polybutadiene, 4.50 mol % branch points,  $M_w = 1.8 \times 10^5$ ;  $\times$ , linear polyethylene,  $M_w = 470\,000$ . Initial level of crystallinity approximately 5% for all samples.  $45^\circ T_m = T_c$  line is also indicated.

crystals. The higher melting peak was associated with the melting of recrystallized material formed during the heating process. In studying very low molecular weight poly(tetramethylene oxide) polymers, Roland and Buckley<sup>55</sup> found that the experimental  $T_m/T_c$  plot paralleled the  $T_m = T_c$  line. Since the level of crystallinity of the samples studied was not specified, it is difficult to attempt an interpretation of these results. Polyethylene sebacates of relatively low molecular weight also presented  $T_m/T_c$  plots that paralleled the  $T_m = T_c$  line in the high-temperature region. No explanation was offered for this unusual behavior.<sup>56</sup>

The extrapolation of the observed melting temperatures to the line  $T_m = T_c$  has apparently been successfully used with many different homopolymers in order to obtain the equilibrium melting temperature.<sup>47,48-52,57-59</sup> However, only in a few cases has the level of crystallinity deliberately been kept low so as to comply with the theoretical requirements. Differences of at least 3–4  $^\circ\text{C}$  are found between the extrapolated melting temperatures of low and high levels of crystallinity.<sup>50,52</sup> This extrapolation method has also been carried for other copolymers with apparent success.<sup>60,61</sup> However, with just one exception,<sup>62</sup> the crystallinity levels were not controlled and can be presumed to have been at convenient high levels.

**Table III**  
Samples Used for  $T_m$ - $T_c$  Experiments (Varying  $(1 - \lambda)$ ) in Figure 3

ethylene copolymer	mol % branch pts	percentage crystallinity <sup>a</sup>	theor equil $T_m^b$	extrapolated $T_m$	slope
ethylene-1-octene (EOA1)	0.69	5	143		1
	0.69	15		154	0.68
branched PE	1.01	5	142		1
high P (A5)	1.01	10–20		>165	0.93
	1.01	30		135	0.64
HPBD (P108)	2.20	5	137.6		1
HPBD (P108)	2.20	15		>165	0.95

<sup>a</sup> Calculated from heat of fusion measurements. <sup>b</sup> Calculated from Flory's equilibrium theory for random copolymers:  $(1/T_m) - (1/T_m^\circ) = (-R/\Delta H_u) \ln p$ ; ( $T_m^\circ = 145.5^\circ\text{C}$ ,  $\Delta H_u = 960\text{ cal/mol}$ ).

The  $T_m/T_c$  method has been extensively used to obtain what has been thought to be equilibrium melting temperature of copolymers. On the basis of our present results, we have examined this method in detail for higher levels of crystallinity. Three different ethylene copolymers with branching composition between 0.69 and 2.2 mol % of branch points were studied for this purpose. The characteristics of these copolymers are given in Table III. The melting behavior of the branched, high-pressure polyethylene was analyzed at three different levels of crystallinity,

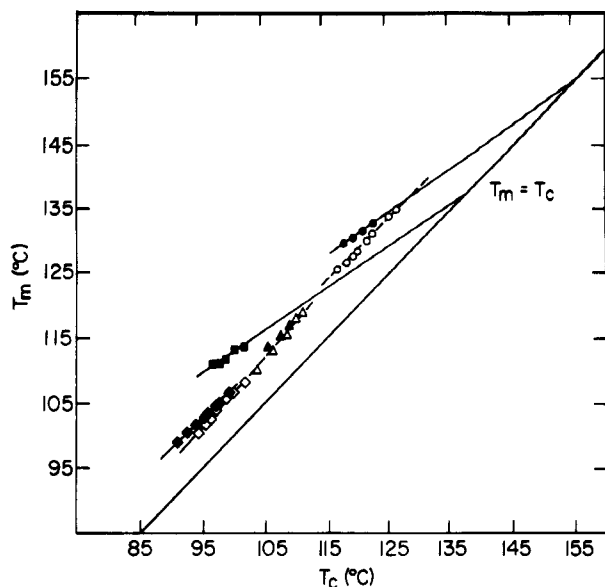


**Figure 3.** Plot of observed melting temperature,  $T_m$ , against crystallization temperature,  $T_c$ , for selected copolymers. These are listed in Table III as are the initial crystallinity levels and extrapolated melting temperatures. Ethylene-octene, 0.69 mol % branch points:  $\circ$ , crystallinity level 5%;  $\bullet$ , crystallinity level 15%. Hydrogenated polybutadiene, 2.2 mol % branch points:  $\diamond$ , crystallinity level 5%;  $\blacklozenge$ , crystallinity level, 15%. High-pressure polymerized polyethylene, 1.01 mol % branch points:  $\Delta$ , crystallinity level 5%;  $\blacktriangle$ , crystallinity level 10–20%;  $\blacksquare$ , crystallinity level 30%.

5, 15, and 30%. To obtain the crystallinity level of 30%, the copolymer had to be crystallized at temperatures close to the nonisothermal crystallization region. The other two copolymers were crystallized to the 15% level, which suffices for present purposes. The observed melting temperatures are plotted against the crystallization temperature in Figure 3. Increasing the level of crystallinity now permits an extrapolation of the data to the 45° line. However, the extrapolation is obviously arbitrary since it depends on the initial level of crystallinity. Consequently, the extrapolated value of  $T_m^\circ$  is also arbitrary. The extrapolated equilibrium melting temperatures are included in Table III. Higher levels of crystallinity results in lower  $T_m/T_c$  slopes and lower extrapolated melting temperatures. A similar behavior was observed with homopolymers.<sup>50,52</sup> Equilibrium melting temperatures calculated from theory<sup>43,44</sup> are also listed in Table III. Depending on the choice of initial level of crystallinity the extrapolated melting temperatures can be greater or less than the theoretical expectation.

We are thus faced with a serious dilemma in determining the true equilibrium melting temperature of random ethylene copolymers by the extrapolative  $T_m/T_c$  method. This raises a serious question as to the use of this extrapolation to determine the equilibrium melting temperature of other type random copolymers. This restraint and concern also holds for stereoirregular polymers, such as the polypropylenes.<sup>64</sup> They are properly treated as copolymers from the point of view of crystallization behavior.

Before attempting to explain these unusual findings, it is informative to examine the underlying theoretical basis for this extrapolation method. The method, although simple in principle, involves some very important assumptions. One starts with the Gibbs–Thompson equation and the inherent assumption that the lateral dimensions of the crystallite are much greater than its thickness. Hence, the melting temperature,  $T_m$ , of the finite size

crystallite can be expressed as

$$T_m = T_m^\circ [1 - 2\sigma_{ec}/\Delta H_u l] \quad (2)$$

Here  $T_m^\circ$  is the equilibrium meeting temperature of the infinite sized crystallite,  $l$  is the crystallite thickness with melting temperature  $T_m$ ,  $\Delta H_u$  is the enthalpy of fusion per repeating unit, and  $\sigma_{ec}$  is the interfacial free energy characteristic of the interphase. Equation 2, based solely on thermodynamic principles, has general applicability to both monomers and polymers. It does not depend on any specific surface structure and, in the case of polymers, has nothing to do with folded chains as has often been implied.<sup>47</sup> The crucial step in the theoretical development is relating  $l$  to the critical size nucleus  $l^*$ . This involves specifying a particular nucleation process and the changes that take place in  $l^*$  and in the interfacial free energy during the development of the critical nucleus to the mature crystallite. As an example, consider in detail the formation of a coherent two-dimensional nucleus of the type first discussed by Gibbs.<sup>65</sup> In this case

$$l^* = 2\sigma_{en} T_m^\circ / \Delta H_u (T_m^\circ - T_c) \quad (3)$$

Here  $\sigma_{en}$  is the interfacial free energy associated with forming a nucleus of critical size. This free energy will in general differ from  $\sigma_{ec}$ . For polymers,  $\sigma_{en}$  or  $\sigma_{ec}$  represents the excess free energy associated with the diffuse interfacial region or interphase that is characteristic of the boundary between the crystalline and liquidlike regions.  $T_c$  is the crystallization temperature. In using eqs 2 and 3, attention is focused solely on changes that are related to the crystallite. The tacit assumption is made that the free energy of fusion per repeating unit, from which  $\Delta H_u$  is obtained, is independent of the level of crystallinity and that the structure of the melt is independent of the crystallinity level and temperature.<sup>66</sup> This assumption is valid for homopolymers, except for those of very low molecular weight. However, this is not a valid assumption for random copolymers. In this case the sequence distribution continuously changes with both the crystallinity level and crystallization temperature.<sup>32,44</sup> Hence, the distinct possibility exists that the apparent melting temperature,  $T_m$ , will change for this reason. It will be further augmented by the Gibbs–Thompson equation and crystallite properties as embodied in the quantity  $l$ . However, we proceed in the analysis by first considering the influence of  $l$  on the apparent melting temperature.

By assuming that  $l = l^*$  and  $\sigma_{ec} = \sigma_{en}$ , the simple relation

$$T_m = T_c \quad (4)$$

is obtained. It was pointed out by Gibbs<sup>65</sup> that a crystallite, even of infinite lateral dimensions, that adheres to these conditions would not be stable at temperatures infinitesimally above  $T_c$ . Therefore, this model is not very useful, either in general or for our specific purpose. However, stability of the mature crystallite can be achieved by allowing  $l$  to increase beyond  $l^*$  with the interfacial free energy fixed. If we allow  $l = ml^*$ , where  $m$  is a constant greater than unity, for all crystallizing temperatures

$$T_m = \frac{(m-1)}{m} T_m^\circ + \frac{T_c}{m} \quad (5)$$

Crystallite stability is thus achieved by this assumption. A linear relation between  $T_m$  and  $T_c$  is obtained with slope  $1/m$ . This type relation is experimentally observed for many homopolymers, with the slope usually being in the range 0.3–0.6. The extrapolation leads to reasonable values of  $T_m^\circ$  when the experiments are carried out at low levels of crystallinity.<sup>50,52</sup> We should note that when  $m = 2$ , eq

5 is identical to that obtained for a three-dimensional nucleation process, with  $l^*$  being the corresponding critical sized nucleus and assuming  $l = l^*$ . In this case stable crystallites result without requiring further growth in the chain direction.<sup>67</sup> The requirements of eq 5 are clearly not met by the experimental data reported here. Neither does a three-dimensional nucleation process hold for the present experimental data.

In a further ramification of eq 2, it is assumed that  $l^* = l$  but  $\sigma_{en}$  does not equal  $\sigma_{ec}$ . The result is that

$$T_m = T_m^\circ(1 - \beta) + \beta T_c \quad (6)$$

where  $\beta = \sigma_{ec}/\sigma_{en}$ . Combining the two cases, namely,  $l = ml^*$  and  $\sigma_{en} \neq \sigma_{ec}$ , leads to the result

$$T_m = T_m^\circ[1 - (\beta/m)] + (\beta/m)T_c \quad (7)$$

Both of these cases lead to linear relations with slopes that differ from unity. Hence the models do not satisfy the present experimental data. Utilizing other types of nucleation processes, but following the same procedure, leads to the same results.

Another approach to this problem, that still focuses sole attention on the properties of crystallites, has been given by Hoffman and Lauritzen.<sup>68</sup> In their analysis of steady-state crystallization kinetics, it is assumed that a two-dimensional coherent nucleus comprised of regularly folded chains was involved. The inherent instability of a crystallite whose thickness was the same as that of a critical sized nucleus was recognized. Since a nucleus comprised of regularly folded chains was assumed, there was no mechanism for the required stability to be achieved by growth along the chain axis. To rectify this situation, average size fluctuations about  $l^*$  were considered. The result was that eq 3 was modified to

$$l^* = \frac{2\sigma_{en}T_m^\circ}{\Delta H_u(T_m^\circ - T_c)} + \delta l \quad (8)$$

where

$$\delta l = kT_c/b_0\sigma \quad (9)$$

Here  $k$  is Boltzmann's constant,  $\sigma$  is the lateral interfacial free energy, and  $b_0$  is the thickness of one layer in the 110 plane. Over the restricted temperature range of isothermal crystallization,  $\delta l$  is essentially a constant. It is estimated to be in the range 5–10 Å for the polyethylenes.<sup>68,69</sup> This procedure suggests that instead of adding a specifically defined quantity  $\delta l$  we add an arbitrary quantity,  $c$ , to  $l^*$  and analyze the results. In effect, instead of multiplying  $l^*$  by a factor independent of crystallization temperature, we add a constant term. By assuming  $\sigma_{ec} = \sigma_{en} \equiv \sigma_e$  and substituting into eq 2, one obtains

$$T_m = T_m^\circ \left[ 1 - \frac{\Delta T}{T_m^\circ} \left( \frac{1}{1 + c\alpha\Delta T/T_m^\circ} \right) \right] \quad (10)$$

Equation 10 is the expression given by Morra and Stein.<sup>70</sup> Here  $\Delta T = T_m^\circ - T_c$  and  $\alpha = \Delta H_u/2\sigma_e$ . In this model  $T_m$  is no longer linear in  $T_c$ . Thus, although stability is gained by adding the constant  $c$  to the thickness of the nucleus, we do not obtain the general result that  $T_m$  is linear in  $T_c$  nor the specific results obtained here, namely, that  $T_m = T_c + k$ .

We can explore the magnitude of the deviation from linearity by expanding the series in eq 10 to obtain

$$T_m = T_c + \frac{c\alpha(\Delta T)^2}{T_m^\circ} - \frac{c\alpha(\Delta T)^3}{T_m^{\circ 2}} + \dots \quad (11)$$

Dalal et al.<sup>71,72</sup> took the analysis one step further by

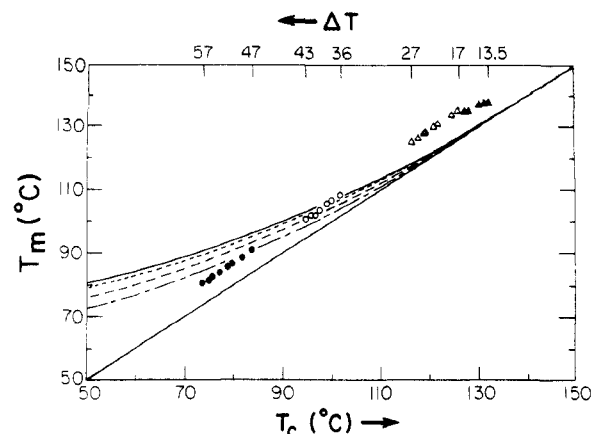


**Figure 4.** Plot of calculated melting temperature against crystallization temperature. Calculations are based on eq 11 with the constant  $c$  set equal to 10 Å. Linear polyethylene (—) and copolymers with 0.7 (---), 2.2 (---) and 4.14 (- - -) branch units per 100 carbons. Experimental results are shown for the following:  $\Delta$ , linear polyethylene;  $\Delta$ , ethylene-octene, 0.69 mol % branch;  $\circ$ , hydrogenated polybutadiene, 2.2 mol % branch points;  $\bullet$ , hydrogenated polybutadiene, 4.14 mol % branch points. Undercooling characteristic of each sample is given on upper abscissa.

allowing  $l^*$  in eq 8 to increase by a factor  $n$  although the nucleus is still comprised of regularly folded chains. Letting  $l = nl^*$  and following the methods given above, there is obtained

$$T_m = T_m^\circ - \frac{\Delta T}{n} [1 - K\Delta T + (K\Delta T)^2 - \dots] \quad (12)$$

where  $K = \Delta H_u \delta l / 2\sigma_e T_m^\circ$ . Equation 12 has the same characteristics of eq 11 and reduces to it for  $n = 1$ .

According to eq 11, the melting temperature, relative to the crystallization temperature, will depend on the quantities  $c$  and  $\alpha$  and also on the equilibrium melting temperature and the undercooling at which the crystallization is conducted. Equation 11 is represented in Figure 4 for some typical samples. These include linear polyethylene and random copolymers containing 0.69, 2.2, and 4.14 mol % branch points, respectively. In this example  $c$  was taken as 10 Å to correspond to  $\delta l$ . The equilibrium melting temperature of linear polyethylene was taken as 145.5 °C.<sup>50,73</sup> The equilibrium melting temperatures of the copolymers were calculated from theory.<sup>43,44</sup> The other parameters were  $\Delta H_u = 2.8 \times 10^9$  erg/cm<sup>3</sup> and  $\sigma = 100$  erg/cm<sup>2</sup>. For these parameters, and the range of crystallization temperatures of interest, the third and higher terms in eq 11 are negligible. The curves in Figure 4 differ from one to the other because of the change in  $T_m^\circ$  with co-unit content. The curvature of the theoretical curves are quite evident. However, each of them approaches linearity as  $T_m^\circ$  (the  $T_m = T_c$  straight line) is approached.

Also plotted in Figure 4 are the experimentally determined melting temperatures for each of the polymers. The undercoolings at which the crystallizations were conducted are also indicated. We can note immediately that the experimentally observed linearity of  $T_m$  with  $T_c$ , with a slope of unity, is not explained by the theoretical curves. With the exception of the 2.2 mol % copolymer, the actual melting temperatures differ significantly from the theoretical prediction. For example, for the 4.14 mol % copolymer a  $c$  value of 10 Å is too high since it overestimates the melting temperature. The value of  $c$  would have to be severely reduced to predict the correct range of melting temperatures. In contrast, to obtain melting temperatures comparable to the experimental ones, values of  $c$  between 37 and 93 Å are needed for the 0.69 mol % copolymer and



between 45 and 107 Å for the linear polyethylene. The closeness of the predicted melting temperature to the actual ones, for the 2.2 mol % copolymer, is fortuitous. We conclude, therefore, that eq 11 cannot be used to explain the results that cover the range from homopolymers and copolymers. Consequently, the premises upon which the equation are based are not valid.

Recently published results<sup>60</sup> have also been analyzed taking into account the above considerations. Unfortunately, the level of crystallinity used in the  $T_m/T_c$  extrapolations was not specified by the authors. Therefore, the validity of the  $T_m^\circ$  cannot be assessed. If eq 11 is to be used to analyze the experimental data, the critical sized nucleus has to thicken to between 25 and 200 Å to satisfy the observations.

In examining the reported results for linear polyethylene,<sup>50</sup> one finds that if eq 11 is used, with  $\delta l \approx 10$  Å, the difference between  $l^*$  and the crystallite thickness calculated to satisfy the experimental  $T_m$  values, 45–107 Å, has to be interpreted as coming from thickening at the isothermal crystallization temperature. However, the  $T_m$ 's were determined at very low levels of crystallinity, about 5%.<sup>50</sup> Hence, achieving the required amount of isothermal thickening would appear to be highly unlikely. On the other hand, the linear extrapolation of  $T_m$  yields  $T_m^\circ$  values in accord with other types of extrapolation.<sup>74,75</sup> For the copolymers the isothermal thickening requirements vary from 0 to 90 Å depending on the polymer and undercooling. In summary the formalism outlined cannot explain either the values of  $T_m$ , for both homopolymers and copolymers, or the slope in the  $T_m/T_c$  plot. Either substantial isothermal thickening must occur or a different nucleation mode is operative.<sup>49</sup> Involving other nucleation modes such as a three-dimensional one, or variants thereof, can explain a large amount of the available data for homopolymers. However, when similar analysis is applied to the copolymers studied here, we do not obtain the result that  $T_m = T_c + k$ .

We have pointed out earlier that the basic analysis that is conventionally used and which we have outlined focuses attention solely on the properties of the crystallite. This is probably a valid procedure for homopolymers. However, for copolymers the thermodynamic properties of the melt change with crystallinity level and temperature. The reason is that the chemical potential of a repeating unit in the melt depends on the sequence distribution of the units rather than directly on composition.<sup>76</sup> As different length sequences crystallize, the concentration of a given length is progressively depleted. The free energy of a unit in the liquid phase will be altered accordingly. This process has been established for equilibrium conditions and is the basis for the broad fusion range of random copolymers.<sup>44</sup> Although it is difficult to quantify this concept for nonequilibrium situations, changes in the chemical potential with the crystallization temperature should occur for this reason. One can expect a contribution from this source to the  $T_m/T_c$  relation which could cause, in part, the experimental observations depicted in Figure 2.

Because of the lack of success in obtaining equilibrium melting temperatures by the extrapolation method, dilatometric studies were undertaken in an attempt to approach equilibrium melting conditions. Some of hydrogenated polybutadiene samples that were used to determine the melting temperatures given in Figure 1 were also used in the dilatometric studies. A set of isothermal crystallization temperatures were used for each fraction. The temperature range for the isothermal crystallization was limited only by the time restraints imposed by the crystallization

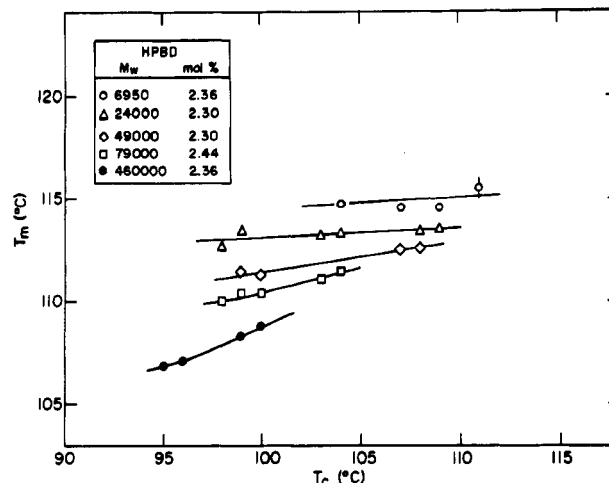


Figure 5. Plot of dilatometrically determined melting temperature (slow heating) against crystallization temperature for a set of hydrogenated polybutadienes. Characteristics of the copolymers are listed.

kinetics.<sup>32</sup> After the initial isothermal crystallization, the dilatometers were heated at the rate of 10 °C/h or somewhat lower, in an effort to approach conditions close to equilibrium. The adoption of slow heating rates results in a substantial amount of melting and recrystallization as the temperature is raised. Therefore, the melting temperatures that are obtained by this procedure are not appropriate to use for the extrapolation method described.

The melting temperatures that were obtained by dilatometry are plotted against the crystallization temperatures,  $T_c$ , in Figure 5. There is an overlap in the crystallization temperatures among most of the fractions. However, the highest crystallization temperatures that could be practically attained progressively decreased with increasing molecular weight. Thus, the lowest undercooling that could be attained for isothermal crystallization was not the same for each of the fractions. This effect is most marked with the highest molecular weight fractions. The data in Figure 5 indicate that compared to the calorimetric results (see Figure 1) the difference in melting temperatures between the molecular weights has become much smaller, particularly after crystallization at the higher temperatures. Although the difference in melting temperatures has become smaller, the inversion with respect to molecular weight is still observed. The trend in the plots in Figure 5 indicate that if crystallization at still lower undercoolings could be carried out, the resulting melting temperatures of the different fractions would become closer. This expectation is particularly evident for the two highest molecular weight fractions.

The experimental and theoretical restraints inherent to random copolymers have hindered both the extrapolation and direct approach to the equilibrium melting temperature. To further understand the melting temperature–molecular weight relation, it is necessary to examine the phase structure of the copolymers.

**Phase Structure.** The relative amounts of the liquidlike, crystalline, and interfacial regions have been determined from density and enthalpy of fusion measurements, as well as from analyses of the Raman internal modes.<sup>2,77</sup> The results for the hydrogenated polybutadienes with about 2.3 mol % ethyl branches and molecular weight ranging between 2200 and 420 000, listed in Table I, are summarized in Figures 6–8. In Figure 6  $(1 - \lambda)_d$ , the crystallinity level from density  $(1 - \lambda)_{dH}$  that from enthalpy of fusion and  $\alpha_c$  the crystallinity level from analysis of the Raman internal modes are plotted for the samples

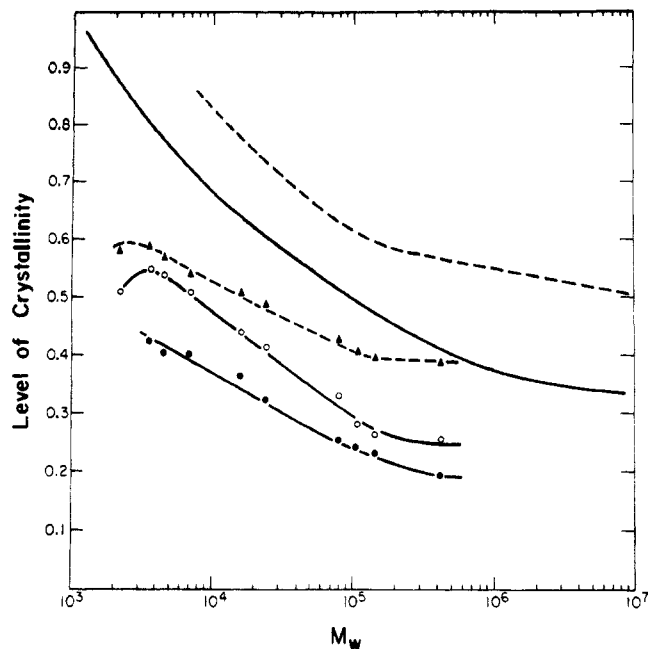


**Figure 6.** Plot of level of crystallinity against log of molecular weight. Linear polyethylene fractions: ---,  $(1-\lambda)_d$  from ref 3; —,  $(1-\lambda)_{\Delta H}$  from ref 78. Hydrogenated polybutadienes, 2.3 mol % branch points (this work):  $\Delta$ ,  $(1-\lambda)_d$ ;  $\circ$ ,  $(1-\lambda)_{\Delta H}$ ;  $\bullet$ ,  $\alpha_c$ .

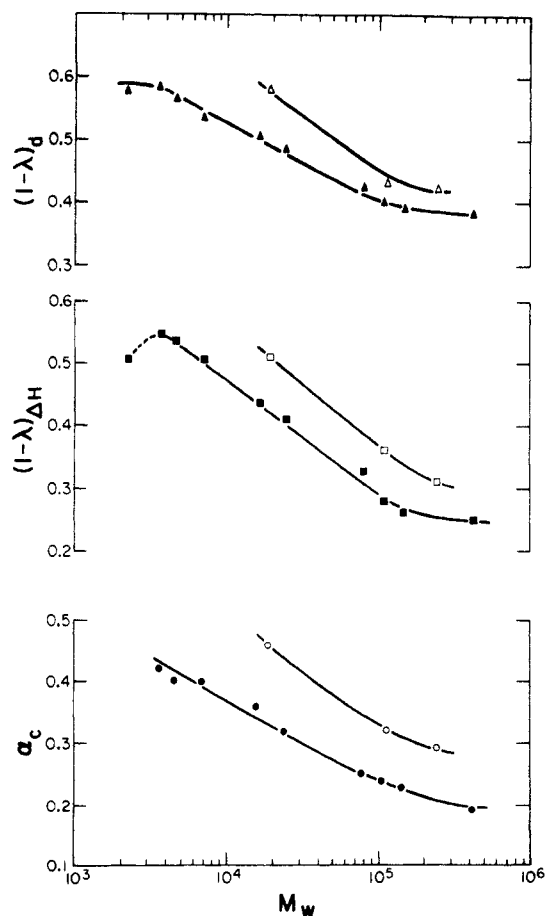


**Figure 7.** Comparison of crystallinity level between hydrogenated polybutadienes, 2.3 mol % branch points, and ethylene-hexene copolymers, 1.47 mol % branch points, as a function of molecular weight.  $(1-\lambda)_d$ :  $\Delta$ , ethylene-hexene;  $\blacktriangle$ , hydrogenated polybutadiene.  $(1-\lambda)_{\Delta H}$ :  $\square$ , ethylene-hexene;  $\blacksquare$ , hydrogenated polybutadiene.  $\alpha_c$ :  $\circ$ , ethylene-hexene;  $\bullet$ , hydrogenated polybutadiene.

quenched to  $-78^\circ\text{C}$ . Also given are previous reported results for  $(1-\lambda)_d$  and  $(1-\lambda)_{\Delta H}$  for quenched linear polyethylene.<sup>3,78</sup> The values of  $\alpha_c$  and  $(1-\lambda)_{\Delta H}$  have been

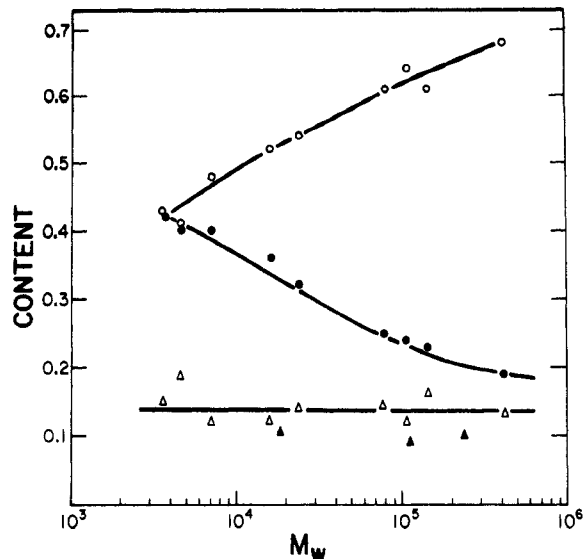


**Figure 8.** Relative amount of phase structure for the hydrogenated polybutadienes as a function of molecular weight:  $\circ$ ,  $\alpha_a$ ;  $\bullet$ ,  $\alpha_c$ ;  $\Delta$ ,  $\alpha_b$ ;  $\blacktriangle$ ,  $\alpha_b'$  for ethylene-hexene copolymers.

shown to be virtually identical for the polyethylenes.<sup>2</sup> The differences between  $(1-\lambda)_d$  and  $(1-\lambda)_{\Delta H}$  are well-known. The levels of crystallinity for linear polyethylene,<sup>3,78</sup> as well as other homopolymers,<sup>5,79,80</sup> are dependent on molecular weight for both isothermal crystallization and by rapid cooling. For the homopolymer, the crystallinity level decreases with increasing molecular weight and appears to level off for molecular weights greater than about  $10^6$ . The ethylene copolymers, with fixed co-unit content, have substantially lower crystallinity levels, for reasons that have recently been discussed in detail.<sup>32</sup> However, the crystallinity decreases with molecular weight in a similar manner. For example, the degree of crystallinity, as measured by  $\alpha_c$ , continually decreases from about 41% for the fraction  $M_w = 6950$  to about 19% for the fraction  $M_w = 4.2 \times 10^5$ . The density and enthalpy of fusion determined crystallinity levels behave in a very similar manner. There is, therefore, a significant decrease in the crystallinity level with increasing molecular weight at a fixed branching content. The data plotted in Figure 6 suggests that the crystallinity level for this set of copolymers will level off at about  $M_w > 5 \times 10^5$ . This suggestion is supported by the results of a copolymer formed by the decomposition of diazoalkanes.<sup>16</sup> Such a copolymer, with a molecular weight of several millions and 2 mol % of propyl branch points, has a  $(1-\lambda)_{\Delta H}$  of 0.24, and  $\alpha_c = 0.22$  in virtual agreement with the asymptotic level of Figure 6. In general, for many aspects of crystallization behavior, the copolymers behaved as though they were of higher molecular weight relative to the behavior of the linear polymer. On the basis of a restricted set of molecular weight data, it was concluded previously that the crystallinity level was independent of chain length, except in the extreme limits, for branched and ethylene copolymers.<sup>81</sup> This conclusion was obviously not correct based on the more extensive data reported here. The molecular weight, particularly in the range  $5 \times 10^4$ – $2 \times 10^5$ , does not play a secondary role in determining the key thermodynamic properties as has been proposed.<sup>82</sup>

Figure 6 also shows that although the three different methods used here for determining the crystallinity levels show the same molecular weight dependence, their magnitude differs from one another by small, but significant, amounts. The Raman internal modes and enthalpy of fusion methods give almost exact agreement for linear polyethylene;<sup>2,8</sup> however,  $(1-\lambda)_{\Delta H}$  is always about 5%



greater than  $\alpha_c$  for the copolymers. The reason is due to the nature of the two different measurements. The copolymers have a broad melting range; hence,  $(1 - \lambda)_{\Delta H}$  includes the contribution of a small amount of crystallinity which has already disappeared at room temperature. The Raman internal modes, being measured at room temperature do not include this contribution. The density determined level of crystallinity  $(1 - \lambda)_d$  is always greater than  $(1 - \lambda)_{\Delta H}$ , or  $\alpha_c$ , for both linear polyethylene and its copolymers. The differences in this case are due to structural reasons and involve the contribution of the interfacial region to  $(1 - \lambda)_d$ . This point will be discussed in more detail shortly.

It has been previously shown that the chemical nature of the branch group (when greater than  $\text{CH}_3$ ) does not influence the crystallinity level when compared at the same branching content and molecular weight. However, the crystallinity level is influenced by the concentration of branches and molecular weight. This point is illustrated in Figure 7, where the crystallinity levels of the 2.3 mol % hydrogenated polybutadienes and the ethylene-hexene copolymers with about 1.4% branch points are compared as a function of molecular weight. The specimens with the lower branch content have larger values of crystallinity level. Despite the differences in branch type and co-unit concentration, the dependence of crystallinity level on molecular weight is almost identical for the two copolymers. They both follow the pattern established by the linear polymer. The data for the copolymer plotted in this figure reinforce the fact that crystallinity levels are sensitive to molecular weight except perhaps in the high molecular weight region  $M \geq 5 \times 10^5$ . Thus, to assess the effect of molecular weight, or copolymer composition, on properties such as melting temperatures or crystallinity levels, it is necessary to hold one of these variables constant.

The results of the Raman internal mode analysis for the hydrogenated polybutadiene samples with 2.3 mol % branch points are given in Figure 8. The plot of  $\alpha_c$  is of course the same as has already been presented in Figures 6 and 7. The plot of the liquidlike content,  $\alpha_a$ , is inverse to that of  $\alpha_c$ , in that it increases with increasing molecular weight. Surprisingly, the interfacial content  $\alpha_b$  remains constant at about 12%, with molecular weight. The previously reported interfacial contents,  $\alpha_b$ , of the ethylene-hexene copolymers,<sup>25</sup> are also given in this figure. For this set of copolymers,  $\alpha_b$  is also invariant with molecular weight but at about the 10% level. These results for the molecular weight dependence of  $\alpha_b$  of copolymers are different from that found for linear polyethylene. For the homopolymer  $\alpha_b$  monotonically increases with molecular weight.<sup>83</sup> For rapidly quenched linear polyethylene fractions  $\alpha_b$  varies from 3 to 16% as the molecular weight increases from  $7 \times 10^3$  to  $8 \times 10^6$ .<sup>83</sup> The invariance in  $\alpha_b$  with molecular weight for the copolymers indicates that the interfacial structure is dominated primarily by the need to accommodate the accumulation of branches on the crystallite surface. This effect is implied by the theoretical simulation of Mattice et al.<sup>84</sup> The effect of the branches dominates the influence of entanglements, which are the major contributors to the molecular weight dependence of the interfacial structure of the linear polymer.<sup>8</sup>

The difference between  $(1 - \lambda)_d$  and  $(1 - \lambda)_{\Delta H}$  in linear polyethylene has been shown to be due to the contribution of the interphase to  $(1 - \lambda)_d$  but not to  $(1 - \lambda)_{\Delta H}$ .<sup>2,8</sup> The density of the interphase is thus very close to that of the core crystallite. A similar result has been reported for ethylene copolymer fractions<sup>25</sup> and further supported by

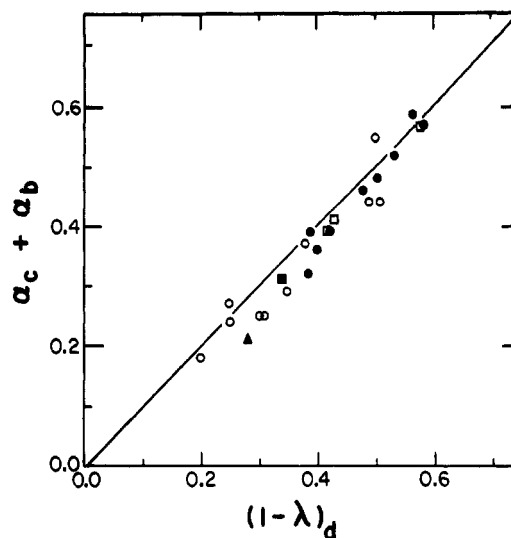
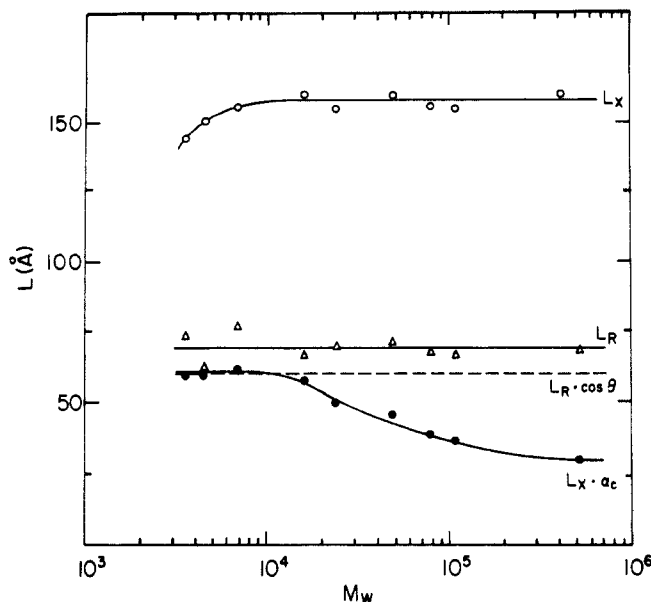


Figure 9. Plot of  $\alpha_c + \alpha_b$ , as determined from the Raman internal modes, against  $(1 - \lambda)_d$  for random copolymers. ●, hydrogenated polybutadienes, ~2.3 mol % branch points (this work); ■, hydrogenated polybutadienes, 4.14 mol % branch points; ▲, hydrogenated polybutadiene, 5.68 mol % branch points; □, ethylene-hexene, 1.47 mol % branch points (this work); ○, other random ethylene copolymers.<sup>17</sup>

the work reported here. These results are illustrated in Figure 9 where the sum  $(\alpha_c + \alpha_b)$  is plotted against  $(1 - \lambda)_d$  for the present data as well as those for other copolymers which were previously reported.<sup>25</sup> Within experimental error all the data quite clearly fall on the 45° line.

Another important property of the phase structure is the thickness of the different regions. The thickness of the core crystallite  $L_c$ , the liquidlike region  $L_a$  and the interfacial region  $L_b$  can be calculated from either the long period, determined by the small-angle X-ray diffraction maxima or from the ordered sequence length determined by the Raman low-frequency longitudinal mode.<sup>12</sup> Either of these methods needs to be used in conjunction with the Raman internal modes. The crystallite thickness and the long period can also be obtained by direct transmission electron microscopy using staining techniques.<sup>35,37</sup>

We focus attention first on calculating the crystallite core thickness. The small-angle long period,  $L_X$ , is plotted against the molecular weight in Figure 10 for the hydrogenated polybutadiene specimens with 2.3 mol % branch points. Surprisingly, except for the two lowest molecular weights  $L_X$  does not vary with chain length. However, the periodicity that is measured includes both the crystalline and noncrystalline regions. Thus to determine  $L_c$ , the crystallite thickness  $L_X$  needs to be multiplied by the crystallinity level. Since the crystallinity levels  $\alpha_c$  and  $(1 - \lambda)_{\Delta H}$  differ from  $(1 - \lambda)_d$ , the question arises as to which one is appropriate in the present problem. In Table IV  $L_X$  is listed in column 3 and  $L_X\alpha_c$  and  $L_X(1 - \lambda)_d$  in the succeeding columns. The crystallite thicknesses, calculated by either of the methods, show the same trend with molecular weight. For both calculations there is a significant decrease in  $L_c$  with increasing molecular weight. However, since  $(1 - \lambda)_d$  is always greater than  $\alpha_c$ , one set of  $L_c$  values is larger than the other. In Figure 10 we have also plotted  $L_c = L_X\alpha_c$ . At the very low molecular weights the crystallite thickness is about 60 Å. However, at about  $M = 10^4$  a precipitous drop occurs and  $L_c$  reaches a value of about 30 Å at  $M_w = 4.2 \times 10^5$ . We should note that this result is quite different from the behavior of quenched linear polyethylene. For this polymer different methods give a constant value of  $L_c$  of about 130 Å over the molecular weight over the range  $10^4$ – $10^6$ .<sup>15,85</sup>



**Figure 10.** Plot of sizes against  $\log M_w$  for hydrogenated polybutadienes: O, long period from small-angle X-ray scattering,  $L_X$ ; ●, crystallite thickness from small-angle X-ray scattering,  $L_X \alpha_c$ ; Δ, most probable value of ordered sequence length from Raman LAM,  $L_R$ ; ---, crystallite thickness from Raman LAM,  $L_R \cos \theta$ ,  $\theta$  taken as  $30^\circ$ .

The ordered sequence length, which can be related to the core crystallite thickness, can also be calculated from the Raman LAM. We follow the procedure that has been successfully used for linear polyethylene. We apply the Scherer-Snyder correction to the data and use eq 1, the simplified Shimanouchi relation, with  $E_c = 2.9 \times 10^{12}$  dyn/cm<sup>2</sup>.<sup>86,87</sup> The results are listed in Table IV and yield a value of  $L_R$  of about 70 Å which is invariant with molecular weight, as is indicated in Figure 10. By correcting for the chain tilt,  $L_R$  can be converted to  $L_c$  by the relation  $L_c = L_R \cos \theta$ . Taking a chain tilt of  $30^\circ$ , the corrected values were calculated and are illustrated by the dashed horizontal line in Figure 10. At the lower molecular weights  $L_R \cos \theta$  gives essentially the same value as was obtained for  $L_c$  from the small-angle X-ray measurement when corrected with  $\alpha_c$ . However, as the molecular weight increases the invariance in  $L_c$  obtained from the Raman LAM is incompatible with the X-ray results. We must therefore decide which method gives the correct values for  $L_c$  and the reason for the significant difference between the two methods.

To resolve the dilemma posed by these contradictory results, we have examined several samples by thin-section transmission electron microscopy. The micrographs are shown in Figure 11, and the quantitative results are listed in the last column of Table IV. The electron micrographs were obtained with the same material that was used for the small-angle X-ray measurements. Thin lamellar crystallites are clearly observed for the copolymers illustrated. They, however, become thinner and more curved with the higher molecular weight. We have previously presented electron micrographs of a copolymer in this series, with  $M_w = 108\,000$ .<sup>36</sup> The lamellar character of the crystallites is lost at this molecular weight under the same crystallization conditions. It was reported as having very small crystallites. Similarly, the electron micrographs of the copolymer with  $M_w = 420\,000$  do not show any definitive lamellar organization. These kinds of results are expected when the crystallite thickness is the order of 30 Å or less. The electron microscopy results clearly show a decrease in lamellar thickness with increasing molecular weight. Except for the low molecular weights, the LAM

analysis carried out does not give the correct results. Possible reasons for this discrepancy will be discussed later. In contrast to this discrepancy the electron microscopy results show the same molecular weight dependence of  $L_c$  as the small-angle X-ray method (compare fourth and last columns of Table IV). Moreover, good quantitative agreement is found between the electron microscopy crystallite thicknesses and those obtained from the long period corrected by the crystallinity from Raman internal modes to yield the crystallite thickness.

In a previous publication<sup>88</sup> the crystallite thicknesses of hydrogenated polybutadienes having the same molecular weight but varying co-unit content were reported for samples crystallized either from the melt or from dilute solution. The crystallite core thicknesses of the solution crystals were found to vary from 34 to 10 Å, by small-angle X-ray measurement; while the copolymer composition ranged from 2.2 to 5.75 mol % branch points. The Raman LAM, analyzed by conventional methods, gave higher values consistent with the results just described. Electron micrographs are not available for this series of copolymers, crystallized from solution, to enable a more quantitative comparison to be made. The HPBD with 3.2 mol % ethyl branches that was slowly cooled from the melt gave similar values between the different methods as to those that we have found here. However, the electron microscopic crystallite thickness, for the 2.2 mol % sample<sup>36</sup> did not give as good agreement. This discrepancy may be due to the fact that two different slow-cooled specimens were used. One was used with the Raman and X-ray measurements, and the other with the electron microscopy. The slow-cooled crystallization obviously produced crystals in one specimen thicker than in the other.

In addition to the crystallite thickness,  $L_c$ , one can also calculate the thickness of the liquidlike region,  $L_a$ , and the thickness of the interphase associated with either of the basal planes,  $L_b$ . From the long-period and the internal modes data the following relations can be established:

$$L_a = L_X(\alpha_a \rho_t / \rho_a) \quad (13)$$

$$L_c = L_X(\alpha_c \rho_t / \rho_c) \quad (14)$$

$$L_b = [L_X - (L_c + L_a)]/2 \quad (15)$$

were  $\rho_t$  = experimentally measured density of the specimen,  $\rho_c = 1.00$  g cm<sup>-3</sup>, and  $\rho_a = 0.852$  g cm<sup>-3</sup>. The results for the copolymers studied here are plotted in Figure 12 along with the previous results for  $L_c$ . As the core crystallite thickness decreases with increasing molecular weight the thickness of the liquidlike region increases very rapidly, reaching a value of about 120 Å while the crystallite thickness is only about 30 Å. The thickness of the interfacial region, on the other hand, remains constant with molecular weight at about 11 Å. This constancy is consistent with the invariance of the interfacial content.

In comparison, the interphase thickness of linear polyethylene fractions range from 14 to 28 Å over a comparable molecular weight range to that studied here. One might intuitively expect that  $L_b$  of copolymers, being dominated by the need to accommodate the branch units on the crystallite surface, would be larger than for the linear polymer of the same molecular weight. Although  $L_b$  of the copolymer is actually smaller, the situation is reversed when comparison is made on the basis of crystallite thicknesses. For example, the interphase of a linear polyethylene fraction with a molecular weight of 10 500 represents only 11% of the total thickness of the crystallite while the interphase of a linear fraction of 425 000 represents 18% of the thickness of its crystal. On

Table IV  
Structural Properties of Hydrogenated Polybutadienes (2.3 mol %) Rapidly Quenched to  $-78^{\circ}\text{C}$

designation (as Table I)	$T_m$ ( $^{\circ}\text{C}$ )	$L_X$ ( $\text{\AA}$ )	$L_X\alpha_c$ ( $\text{\AA}$ )	$L_X(1-\lambda)_d$ ( $\text{\AA}$ )	$L_R$ ( $\text{\AA}$ )	$L_R \cos 30$ ( $\text{\AA}$ )	$L_E$ ( $\text{\AA}$ )
HPBD-35800	106.2	144	60	84	74	64	
HPBD-4530	107.3	151	60	85	63	55	
HPBD-6950	106.4	156	68	91	77	67	$54.5 \pm 10$
P-16	103.1	160	58	81	67	58	
HPBD-24	103.6	155	50	75	70	61	$46.6 \pm 8$
HPBD-49	(102) <sup>a</sup>	160	46	70	72	62	
HPBD-79	101.8	156	39	66	68	59	
P108	100.0	155	37	62	67	58	very small crystals
P420	100.2	160	30	61	69	60	very small crystals
P108 SC <sup>(b)</sup>		170	46	70	100	87	$70 \pm 14$
HPBD-4 SC <sup>(b)</sup>		170	31	65	53	46	$40 \pm 8$

<sup>a</sup> Interpolated from Figure 1. <sup>b</sup> Samples slow cooled from the melt. Data from refs 88 and 36.

the other hand, the interphase of the hydrogenated polybutadiene with a molecular weight of 16 000 represents 17% of the core crystalline thickness. The interface of the copolymer with 420 000 represents 37% of the crystallite thickness. Therefore, relative to the total crystallite, copolymers with 2.3 mol % branch units possess interphases that are about twice those of the linear polymers.

Figure 12 illustrates an interesting point that at the higher molecular weights the small core crystallite thickness of about 30  $\text{\AA}$  supports a disordered overlayer that is about 4 times as thick. This conclusion is supported by the measured crystallinity levels and the electron micrographs. Similar results have been obtained with hydrogenated polybutadienes crystallized from dilute solution as well as for isotactic polystyrene and isotactic polypropylene.<sup>88</sup> Although initially surprising, these results are self-consistent. For a quenched high molecular weight linear polyethylene the average crystallite thickness is about half that of the long period.<sup>85</sup>

The fact that the crystallite thickness decreases with molecular weight is consistent with the observation that the melting temperature also decreases with molecular weight (Figure 1). These results can explain the unexpected melting temperature observation if the interfacial free energies,  $\sigma_{ec}$ , characteristic of the basal planes of the mature crystallites did not vary very much with molecular weight. Using the Thompson-Gibbs equation, eq 2,  $\sigma_{ec}$  can be calculated from the data in Table IV. We have used  $\Delta H_u = 2.8 \times 10^9 \text{ erg/cm}^3$ <sup>29</sup> and  $T_m^{\circ} = 137.1^{\circ}\text{C}$  calculated from equilibrium theory.<sup>43,44</sup> The values of  $\sigma_{ec}$  determined in this manner are plotted in Figure 13. Within the experimental error there is a small decrease in  $\sigma_{ec}$  with increasing molecular weight. The reason for this slight decrease in  $\sigma_{ec}$  is not clear at present. It could be due to several causes. Among those are the possibilities of chain tilting and lattice expansion with molecular weight. Nevertheless, the data make clear that the major reason for the decreased melting temperature with increased molecular weight is the decreasing crystallite thickness. Other factors such as imperfection within the crystallites may also contribute to this dependence.

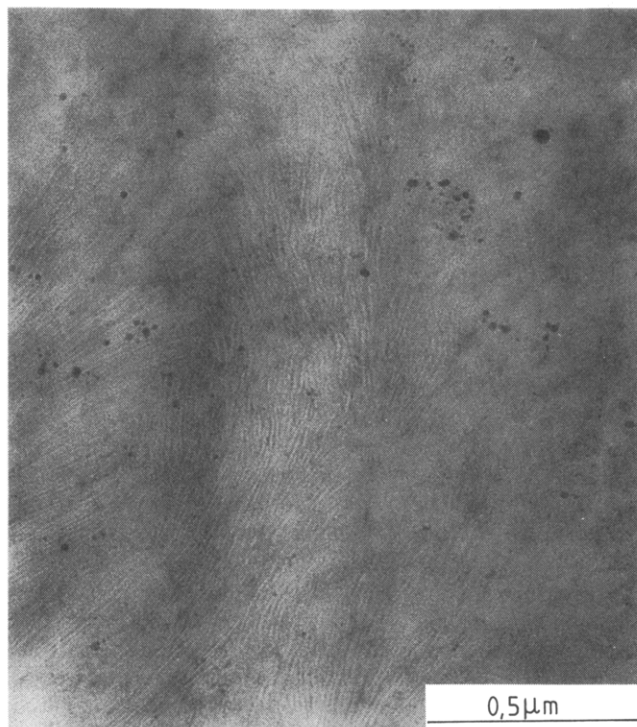
It is of interest to theoretically explore the magnitude of the crystallite thickness and its molecular weight dependence. This size is determined by the thickness of the critical nucleus  $\xi^*$  and its subsequent growth to a stable mature crystallite. For purposes of exploring the basis for the crystallite thickness, we have calculated the critical nucleus size for a coherent two-dimensional Gibbs type nucleus using finite chain theory and reasonable values for the interfacial nucleation free energy.<sup>32</sup> The calculations were carried out for the lowest temperature at which the crystallization process is isothermal. This temperature is known from previous studies of the crystallization

kinetics of the same copolymers.<sup>32</sup> This temperature decreases with increasing molecular weight. Since the samples studied here were rapidly crystallized, this temperature should serve as upper limit to the actual crystallization temperature and thus to  $\xi^*$ .

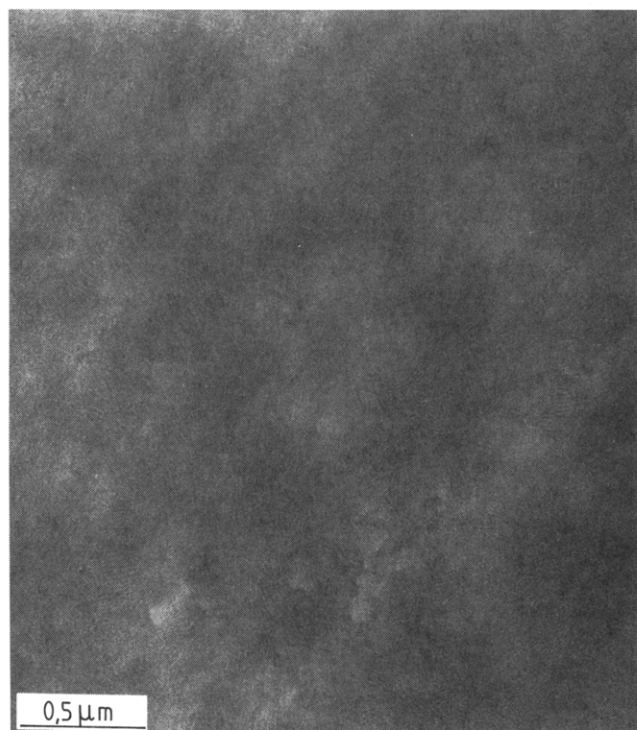
The values of  $\xi^*$ , calculated in the manner outlined, are plotted in Figure 14 for  $\sigma_{en}$  values of 2000, 1500, and 1000 cal/mol of sequences. The specific nucleation theory that was selected for analysis predicts a similar molecular weight dependence between the observed  $L_c$  and the calculated  $\xi^*$ . Their orders of magnitude are also close to one another. However, despite their qualitative similarities for  $\sigma_{en} = 2000 \text{ cal/mol}$ ,  $\xi^*$  is greater than  $L_c$  for all molecular weights. This is of course an impossible physical situation. When  $\sigma_{en}$  is lowered to 1500 cal/mol,  $\xi^*$  will of course be reduced. At the lower molecular weights, for this value of  $\sigma_{en}$ ,  $\xi^*$  is 5–10  $\text{\AA}$  less than  $L_c$ . At the higher molecular weights  $\xi^*$  again exceeds  $L_c$ . If, however,  $\sigma_{en}$  is reduced to 1000 cal/mol, then  $\xi^*$  is less than  $L_c$  while maintaining a similar molecular weight dependence. For this situation  $\sigma_{ec}$  would be greater than  $\sigma_{en}$ . The actual temperature which governs the crystallization (and nucleation) is probably less than the lower isothermal limit used in the calculation because of the rapid cooling that is involved. The result would be a reduction in the size of the critical nucleus. This qualitative analysis indicates that there is a distinct possibility that  $L_c$ , and its molecular weight dependence, is determined primarily by  $\xi^*$ . Growth along the chain axis must take place for stability to be achieved with this nucleation mode. This would be expected to be a slow process for random copolymers. A quantitative calculation of the crystallite thickness is difficult because of the inability to specify the actual crystallization temperature, the specific nucleation mode that is operative and the exact value of the interfacial free energy that is involved.

In a previous report the thicknesses of the different regions were given for a series of hydrogenated polybutadienes that were rapidly crystallized from dilute solution.<sup>88</sup> The copolymers studied had a fixed molecular weight of about  $1 \times 10^5$  and a branch point concentration that ranged from 2.2 to 6 mol %. The results are plotted in Figure 15 along with the data for linear polyethylene of similar molecular weight crystallized under the same conditions. The interfacial thickness increases from 5  $\text{\AA}$  for the linear polymer to about 11  $\text{\AA}$  for the copolymer having the highest co-unit content. The crystallite thickness, calculated from the long period, decreases rapidly from about 80–90 to about 10  $\text{\AA}$  as the branch content increases. Concomitantly, the disordered overlayer increases from 16 to 89  $\text{\AA}$ .

Wilke et al. have reported small- and wide-angle X-ray scattering data for ethylene-butene fractions crystallized from the melt.<sup>89</sup> The molecular weight and co-unit content



(a)



(b)

**Figure 11.** Thin-section transmission electron micrographs of rapidly crystallized hydrogenated polybutadienes: (a)  $M_w = 6950$ ; (b)  $M_w = 24\,000$ .

of the fractions were not treated as independent variables. The thicknesses of the lamellae were calculated according to a one-dimensional paracrystalline model and were found to be independent of the degree of branching. However, if the experimental values of the long period reported by these authors are corrected by the given crystallinity levels,

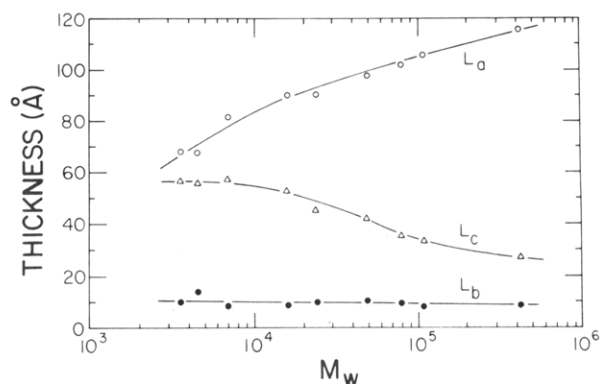


**Figure 12.** Thicknesses of different regions as a function of  $\log M_w$ , for rapidly crystallized hydrogenated polybutadienes.  $\Delta$ , crystallite core thickness  $L_c$ ;  $\circ$ , liquidlike region  $L_a$ ;  $\bullet$ , interfacial region  $L_b$ .

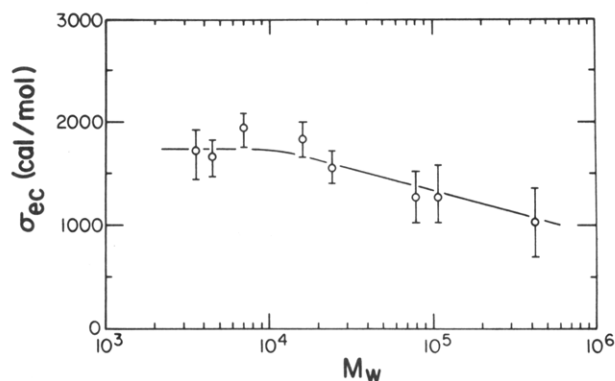


**Figure 13.** Interfacial surface free energies of crystallites of rapidly crystallized hydrogenated polybutadienes plotted against  $\log M_w$ .

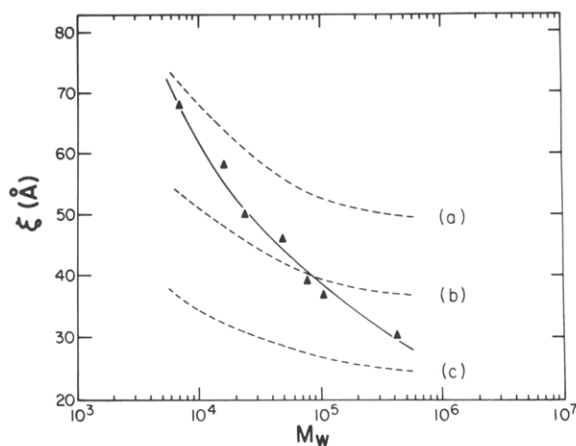


**Figure 14.** Comparison of observed crystallite thicknesses (—) with critical nuclei dimensions, calculated from finite chain two-dimensional theory (---) for hydrogenated polybutadienes: (a)  $\sigma_e = 2000$  cal/mol; (b)  $\sigma_e = 1500$  cal/mol; (c)  $\sigma_e = 1000$  cal/mol.  $\Delta$ , experimental crystallite thicknesses ( $L_X\alpha_c$ ).

the lamellae thicknesses decrease rapidly with increasing co-unit content in agreement with our results.<sup>88</sup>

Of particular interest in the present context is the comparison between the crystallite thickness determined by the Raman LAM and the small-angle X-ray maxima. The difference between the two methods is similar to that found for the bulk crystallized hydrogenated polybutadienes. For the homopolymers there is good agreement between the two methods. However, as the co-unit content increases, and the crystallite sizes decrease, a major difference develops between them. As in the bulk crystallized case the Raman LAM gives larger values for the

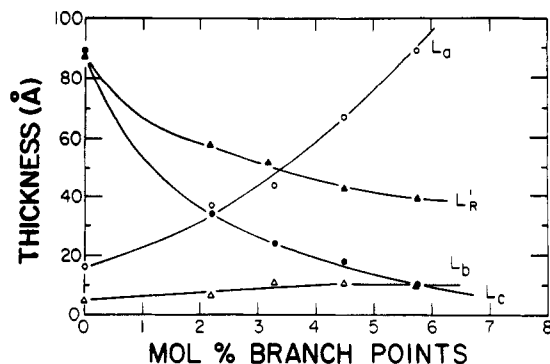


Figure 15. Plot of size against  $\log M_w$  for hydrogenated polybutadienes crystallized from dilute solution: O, liquidlike region,  $L_a$ ; crystallite thickness from Raman,  $L'_R \cos 30^\circ$ ; ●, crystallite thickness from small-angle X-ray scattering  $L_c$ ; Δ, interfacial thickness,  $L_b$ . Data from ref 88.

crystallite thickness.

The reason that the two methods do not agree is not clear. Several possibilities suggest themselves. Because of the relatively high proportion of the interfacial structure, the use of eq 1 and the "free elastic rod" model may not be correct. The non-ordered surface may have an important influence on the vibration of the ordered sequences in the crystal. However, applying the segmented rod model<sup>90,91</sup> to the spectral data further enhances the disparity. Use of second and higher terms in the Shimanouchi-Schaufele formulation,<sup>40</sup> of which eq 1 is the first term, also brings the results farther apart. Analyzing the Raman LAM spectra by the method of Snyder and Scherer<sup>41</sup> yields a broad distribution of ordered sequence lengths and thus of crystallite thicknesses. We know from previous works that different methods do not always yield the same average value for the crystallite size when dealing with broad distributions.<sup>92</sup> This problem will be further compounded when dealing with very small ordered sequence lengths.

## Conclusion

Several different directions have been taken to explain the decrease in melting temperature that is observed with molecular weight for the random copolymers with fixed co-unit content. In an effort to obtain equilibrium melting temperatures, resort was made to the extrapolative method involving the dependence of the observed melting temperature on the crystallization temperature. This method, which has been universally used for homopolymers, failed in this case for reasons that are not quantitatively understood as yet. The melting temperature was found to be proportional to the crystallization temperature, so that the extrapolation could not be carried out.

Long-time isothermal crystallization at high temperatures that produce thicker and more stable crystals brought the melting temperatures closer to one another. However, the observed  $T_m/M_w$  dependence was still maintained.

Different methods of analysis of the level of crystallinity all followed the same pattern with molecular weight as observed for linear polyethylene. The level of crystallinity decreases with increasing molecular weight due to the increased entanglement concentration of the original melt. The interfacial content, on the other hand, is independent of molecular weight.

Attention was also directed to a study of the phase structure and the crystallite thickness. For the first time, the dependence of the phase structure with molecular weight, at a fixed branching content, as well as with co-unit content for a fixed molecular weight were indepen-

dently analyzed for the copolymer fractions crystallized from either the melt or solution. Very small core crystallite thicknesses were found for the highest molecular weights and for the high co-unit content analyzed. The core crystallite thickness decreased with increasing molecular weight. The crystallite size was shown to be the major reason for the decreased melting temperature. It was also found in the work that the Raman LAM did not give crystallite sizes that were in agreement with those determined by either thin-section electron microscopy or small-angle X-ray scattering. This discrepancy can be attributed to the very small crystallite size and the concomitant large disordered overlayer.

The observed dependence of properties with molecular weight is not qualitatively altered by either the chemical nature of the branch or the co-unit concentration.

**Acknowledgment.** This work was supported by the Polymer Program Grant DMR 89-14167 of the National Science Foundation and the Deutsche Forschungsgemeinschaft SFB41.

## References and Notes

- (1) Mandelkern, L. Organization of Macromolecules in the Condensed Phase. *Discuss. Faraday Soc.* 1979, 69, 310.
- (2) Mandelkern, L. *Polym. J.* 1985, 17, 337.
- (3) Mandelkern, L. *J. Phys. Chem.* 1971, 75, 3909.
- (4) Ergoz, E.; Fatou, J. G.; Mandelkern, L. *Macromolecules* 1972, 5, 147.
- (5) Magill, J. H. *Makromol. Chem.* 1986, 187, 455.
- (6) Maxfield, J.; Mandelkern, L. *Macromolecules* 1977, 10, 1141.
- (7) Mandelkern, L.; Glotin, M.; Benson, R. S. *Macromolecules* 1981, 14, 22.
- (8) Glotin, M.; Mandelkern, L. *Colloid Polym. Sci.* 1982, 260, 182.
- (9) Popli, R.; Glotin, M.; Mandelkern, L.; Benson, R. S. *J. Polym. Sci., Polym. Phys. Ed.* 1984, 22, 407.
- (10) Axelson, D. E.; Mandelkern, L.; Popli, R.; Mathieu, P. *J. Polym. Sci., Polym. Phys. Ed.* 1983, 21, 2319.
- (11) Popli, R.; Mandelkern, L. *J. Polym. Sci., Polym. Phys. Ed.* 1987, 25, 441.
- (12) Mandelkern, L.; Alamo, R. G.; Kennedy, M. A. *Macromolecules* 1990, 23, 4721.
- (13) Allen, R. C.; Mandelkern, L. *J. Polym. Sci., Polym. Phys. Ed.* 1982, 20, 1465.
- (14) Allen, R. S., Ph.D. Dissertation, School of Materials Engineering Sciences, Virginia Polytechnic Institute and State University, 1981.
- (15) Mandelkern, L. *Acc. Chem. Res.* 1990, 23, 380.
- (16) Richardson, M. J.; Flory, P. J.; Jackson, J. B. *Polymer* 1963, 4, 221.
- (17) Alamo, R.; Domszy, R.; Mandelkern, L. *J. Phys. Chem.* 1984, 88, 6587.
- (18) Perez, E.; Vanderhart, D. L.; Crist, B. Jr.; Howard, P. R. *Macromolecules* 1987, 20, 789.
- (19) Laupretre, F.; Monnerie, L.; Barthelemy, L.; Wairon, J. P.; Sanzean, A.; Roussel, D. *Polym. Bull.* 1986, 15, 159.
- (20) McFaddin, D. C.; Russel, K. E.; Kelusky, E. C. *Polym. Commun.* 1986, 27, 204.
- (21) Voigt-Martin, I. G.; Mandelkern, L. *Handbook Polym. Sci. Technol.* 1989, 3, 1.
- (22) We are grateful to Dr. W. W. Graessley for his generosity in supplying us with the HPBD. They are an invaluable set of materials in our studies of the thermodynamic and structural properties of ethylene copolymers.
- (23) Rachapudy, H.; Smith, G. G.; Raju, U. R.; Graessley, W. W. *J. Polym. Sci., Polym. Phys. Ed.* 1979, 17, 1211.
- (24) Kaminsky, W.; Hähnsen, H.; Kulper, K.; Woldt, R. U.S. Patent 4,542,199, 1985.
- (25) Alamo, R. G.; Mandelkern, L. *Macromolecules* 1989, 22, 1273.
- (26) Mandelkern, L.; Maxfield, J. *J. Polym. Sci., Polym. Phys. Ed.* 1979, 17, 1913.
- (27) Randall, J. C. *J. Polym. Sci., Polym. Phys. Ed.* 1975, 13, 1975.
- (28) Randall, J. C. *Macromolecules* 1982, 15, 353.
- (29) Quinn, F. A., Jr.; Mandelkern, L. *J. Am. Chem. Soc.* 1958, 80, 3178.
- (30) Flory, P. J.; Mandelkern, L.; Hall, H. K. *J. Am. Chem. Soc.* 1951, 73, 2532.
- (31) Baker, C. H.; Mandelkern, L. *Polymer* 1966, 7, 7.
- (32) Alamo, R. G.; Mandelkern, L. *Macromolecules* 1991, 24, 6480.

- (33) Chiang, R.; Flory, P. J. *J. Am. Chem. Soc.* **1961**, *83*, 2057.
- (34) Kanig, G. *Prog. Colloid Polym. Sci.* **1975**, *57*, 176.
- (35) Voigt-Martin, I. G.; Fischer, E. W.; Mandelkern, L. *J. Polym. Sci., Polym. Phys. Ed.* **1980**, *18*, 2347. Voigt-Martin, I. G.; Stack, G. M.; Peacock, A. J.; Mandelkern, L. *J. Polym. Sci., Polym. Phys. Ed.* **1989**, *27*, 957.
- (36) Voigt-Martin, I. G.; Alamo, R.; Mandelkern, L. *J. Polym. Sci., Polym. Phys. Ed.* **1986**, *24*, 1283.
- (37) Strobl, G. R.; Schneider, M. J.; Voigt-Martin, I. G. *J. Polym. Sci., Polym. Phys. Ed.* **1980**, *18*, 1361.
- (38) Strobl, G. R.; Hagedorn, W. *J. Polym. Sci., Polym. Phys. Ed.* **1978**, *16*, 1181.
- (39) Mandelkern, L.; Peacock, A. J. *Polym. Bull.* **1986**, *16*, 529.
- (40) Schaefele, R. F.; Shimanouchi, T. *J. Chem. Phys.* **1967**, *47*, 3605.
- (41) Snyder, R. G.; Scherer, J. R. *J. Polym. Sci., Polym. Phys. Ed.* **1978**, *16*, 1593.
- (42) Hser, J. C.; Carr, S. H. *Polym. Eng. Sci.* **1979**, *19*, 436. Mathot, V. B. F.; Pijpers, M. F. *J. Polym. Bull.* **1984**, *11*, 297.
- (43) Flory, P. J. *J. Chem. Phys.* **1949**, *17*, 223.
- (44) Flory, P. J. *Trans. Faraday Soc.* **1955**, *51*, 848.
- (45) This statement is true for ethyl and longer branches. It is well established that directly bonded CH<sub>3</sub> groups enter the crystal lattice.<sup>16,17,19</sup> Hence, a different type of melting temperature-molecular weight behavior would be expected.
- (46) We wish to thank Dr. J. C. Randall for carrying out this analysis for us.
- (47) Hoffman, J. D.; Weeks, J. J. *J. Res. Natl. Bur. Stand. Part A* **1962**, *66*, 13.
- (48) Mandelkern, L. *J. Polym. Sci.* **1960**, *47*, 494.
- (49) Mandelkern, L. *Crystallization of Polymers*; McGraw-Hill: New York, 1964; p 321.
- (50) Gopalan, M.; Mandelkern, L. *J. Phys. Chem.* **1967**, *71*, 3833.
- (51) Fatou, J. G. *Eur. Polym. J.* **1971**, *7*, 1057.
- (52) Beech, D. R.; Booth, C. J. *Polym. Sci., Polym. Lett. Ed.* **1979**, *8*, 731.
- (53) Okui, N.; Kawai, T. *Makromol. Chem.* **1972**, *156*, 161.
- (54) Lee, Y.; Porter, R. S. *Macromolecules* **1987**, *20*, 1336.
- (55) Roland, M. C.; Buckley, G. S. *Rubber Chem. Technol.* **1991**, *64*, 74.
- (56) Theil, M. H.; Mandelkern, L. *J. Polym. Sci., Polym. Phys. Ed.* **1970**, *8*, 957.
- (57) Magill, J. H. *Makromol. Chem.* **1965**, *86*, 283.
- (58) Miller, R. L.; Seeley, E. G. *J. Polym. Sci., Polym. Phys. Ed.* **1982**, *20*, 2292.
- (59) Alamo, R. G.; Bello, A.; Fatou, J. G.; Obrador, C. *J. Polym. Sci., Polym. Phys. Ed.* **1990**, *28*, 907.
- (60) Martinez-Salazar, J.; Sanchez, M.; Balta-Calleja, F. J. *Colloid Polym. Sci.* **1987**, *265*, 239.
- (61) Goulet, L.; Prud'Homme, R. E. *J. Polym. Sci., Polym. Phys. Ed.* **1990**, *28*, 2329.
- (62) The  $T_m$ - $T_c$  procedure was successfully carried out with poly(vinylidene fluoride) at low levels of crystallinity.<sup>63</sup> This copolymer, however, is a special case since a substantial amount of the head-to-head structure enters the crystal lattice.
- (63) Nandi, A. K.; Mandelkern, L. *J. Polym. Sci., Polym. Phys. Ed.* **1991**, *29*, 1287.
- (64) Cheng, S. Z. D.; Janimak, J. J.; Zhang, A.; Hsieh, E. *Polymer* **1991**, *32*, 648.
- (65) Gibbs, J. W. *Collected Works*; Longman, Green and Co.: Essex, UK, 1928.
- (66) The usual changes of the free energy with temperature, involving the specific heat, are of course applicable.
- (67) Although our analysis is given for  $l^*$  resulting from a two-dimensional coherent nucleation process, this is an assumption of convenience. The analysis can be carried out in an analogous manner for three-dimensional nucleation<sup>49</sup> or, in fact, any type of nucleation process.
- (68) Lauritzen, J. I.; Hoffman, J. D. *J. Res. Natl. Bur. Stand.* **1960**, *64A*, 73.
- (69) Mandelkern, L. *Discuss Faraday Soc.* **1979**, *69*, 375.
- (70) Morra, B. S.; Stein, R. S. *J. Polym. Sci., Polym. Phys. Ed.* **1982**, *20*, 2243.
- (71) Dalal, E. M.; Taylor, K. D.; Phillips, P. J. *Polymer* **1983**, *1623*, 1983.
- (72) Dalal, E. N. Ph.D. Dissertation, University of Utah, 1982.
- (73) Flory, P. J.; Vrij, A. *J. Am. Chem. Soc.* **1963**, *85*, 3548.
- (74) Hoffman, J. D.; Lauritzen, J. J.; Passaglia, E.; Ross, G. S.; Frolen, L. J.; Weeks, J. J. *Kolloid Z., Z. Polym.* **1969**, *231*, 564.
- (75) Hoffman, J. D. *Discuss. Faraday Soc.* **1979**, *69*, 469.
- (76) If the crystalline phase did not remain pure, the chemical potential of a unit in this state would also vary.
- (77) Failla, M.; Alamo, R. G.; Mandelkern, L. *Polym. Testing* **1992**, *11*, 151.
- (78) Mandelkern, L.; Allou, A. L., Jr.; Gopalan, M. *J. Phys. Chem.* **1968**, *72*, 309.
- (79) Alamo, R.; Fatou, J. G.; Guzman, J. *Polymer* **1982**, *23*, 374.
- (80) Jadraque, D.; Fatou, J. G. *An. Quim.* **1977**, *73*, 639.
- (81) Mandelkern, L.; Glotin, M.; Benson, R. A. *Macromolecules* **1981**, *14*, 22.
- (82) Springer, H.; Hengse, A.; Hinrichsen, G. *J. Appl. Polym. Sci.* **1990**, *40*, 2173.
- (83) Mandelkern, L.; Peacock, A. J. In *Studies in Physical and Theoretical Chemistry*; Lacher, R. C., Ed.; Elsevier Science Publishers: Amsterdam, 1988; Vol. 54, pp 201-227.
- (84) Mathur, S. C.; Rodriguez, K.; Mattice, W. L. *Macromolecules* **1989**, *22*, 2781.
- (85) Voigt-Martin, I. G.; Mandelkern, L. *J. Polym. Sci., Polym. Phys. Ed.* **1981**, *19*, 1769.
- (86) Strobl, G. R.; Eckel, R. *J. Polym. Sci., Polym. Phys. Ed.* **1976**, *14*, 913.
- (87) Glotin, M.; Mandelkern, L. *J. Polym. Sci., Polym. Phys. Ed.* **1983**, *21*, 29.
- (88) Domszy, R. C.; Alamo, R.; Mathieu, P. J. M.; Mandelkern, L., *J. Polym. Sci., Polym. Phys. Ed.* **1984**, *22*, 1727.
- (89) Heink, M.; Häberle, K. D.; Wilke, W. *Colloid Polym. Sci.* **1991**, *269*, 675.
- (90) Hsu, S. L.; Krimm, S. *J. Appl. Phys.* **1976**, *47*, 4265; **1977**, *48*, 4013. Hsu, S. L.; Ford, G. W.; Krimm, S. *J. Polym. Sci., Polym. Phys. Ed.* **1977**, *15*, 1769.
- (91) Peterlin, A. *J. Appl. Phys.* **1979**, *50*, 838; *J. Mater. Sci.* **1979**, *14*, 2994.
- (92) Voigt-Martin, I. G.; Mandelkern, L. *J. Polym. Sci., Polym. Phys. Ed.* **1989**, *27*, 967.

**Registry No.** Polyethylene, 9002-88-4; ethylene-1-butene, 25087-34-7; ethylene-1-octene, 26221-73-8; ethylenevinyl acetate, 24937-78-8; ethylene-1-hexene, 25213-02-9.